

# Experiments on the Simultaneous Hand-Held Control of Rigid Endoscopes and Robots Passing Through Them

Richard J. Hendrick, S. Duke Herrell, Christopher R. Mitchell  
and Robert J. Webster III

**Abstract** Concentric tube manipulators have the diameter of needles and are consequently amenable to delivery into the human body through small ports in an endoscope. When this is done, the surgeon must manipulate both the endoscope and one or more concentric tube robots simultaneously. In this paper we explore a hand-held approach to this user interface challenge, in which the surgeon has direct physical control of endoscope pose and can use finger and thumb controls to specify the motion of two concentric tube robots that pass through the endoscope. In experiments with the system, we explore whether the endoscope-robot combination can reach locations in the prostate that are inaccessible to the endoscope alone. We also compare joint space and task space control for three-degree-of-freedom concentric tube robots, and demonstrate experimentally that laser resection of prostate tissue is possible using an anthropomorphic phantom.

## 1 Introduction

A great deal of interest in the surgical robotics community is currently focused on enabling less invasive access to the human body through natural orifices. Despite the relatively small diameter of the urethra, it is no exception. In fact, Transurethral Resection of the Prostate (TURP) was one of the earliest surgical robotics applica-

---

R.J. Hendrick (✉) · R.J. Webster III  
Department of Mechanical Engineering, Vanderbilt University, VU Station B 351592,  
2301 Vanderbilt Place, Nashville, TN 37235-1592, USA  
e-mail: richard.j.hendrick@vanderbilt.edu

R.J. Webster III  
e-mail: robert.webster@vanderbilt.edu

S.D. Herrell · C.R. Mitchell  
Department of Urologic Surgery, Vanderbilt University Medical Center,  
A-1302 Medical Center, Nashville, TN 37232-2765, USA  
e-mail: duke.herrell@vanderbilt.edu

C.R. Mitchell  
e-mail: christopher.r.mitchell@vanderbilt.edu

© Springer International Publishing Switzerland 2016  
M.A. Hsieh et al. (eds.), *Experimental Robotics*, Springer Tracts  
in Advanced Robotics 109, DOI 10.1007/978-3-319-23778-7\_6

73

tions [1, 2]. Somewhat surprisingly, since that pioneering work, only a few research groups have developed robotic systems designed for transurethral deployment. In 2001, robotic transurethral laser resection of the prostate through a standard resectoscope was mentioned by Ho et al. [3], though the authors' main focus was on the Nd:YAG laser rather than on the robotic system. In 2002, Badajoz et al. proposed master-slave teleoperation of a robot holding a transurethral resectoscope for prostate resection [4]. In 2004, Hashimoto et al. described a 4 degree-of-freedom (DOF) manipulator intended for prostate resection that delivers a drill and cutter through an 8 mm rigid tube under ultrasound image guidance [5]. A major challenge was the removal of excised tissue from the body, since a morcellator was not incorporated into the intended workflow. In 2013, Goldman et al. demonstrated the feasibility of transurethral robotic bladder access, and simultaneously described the first use of a continuum robot in a transurethral application of which we are aware. Their robot delivered a laser fiber and biopsy forceps for bladder tumor resection [6].

We recently presented a new hand-held surgical robot aimed at improving transurethral prostate surgery by making it easier to perform [7]. Our system follows the continuum robot paradigm of Goldman et al. but uses a different, smaller type of continuum robot called a concentric tube robot, enabling it to deliver two manipulators through a 5 mm diameter port in a standard clinical resectoscope (see Fig. 1). One manipulator aims a holmium laser fiber, and the other provides tissue retraction [7].

This robotic system was motivated by the prospect of increasing the utilization of a procedure that is known to have excellent clinical outcomes, yet has failed to achieve widespread adoption due to its steep learning curve. The procedure is called Holmium Laser Enucleation of the Prostate (HoLEP), and is currently conducted using a straight, rigid endoscope. In this procedure, a holmium laser fiber is passed through the endoscope and used to cut prostate tissue that is obstructing urine flow. HoLEP has been clinically demonstrated to have significantly better outcomes for patients than traditional TURP which uses sharp dissection or electrocautery. These

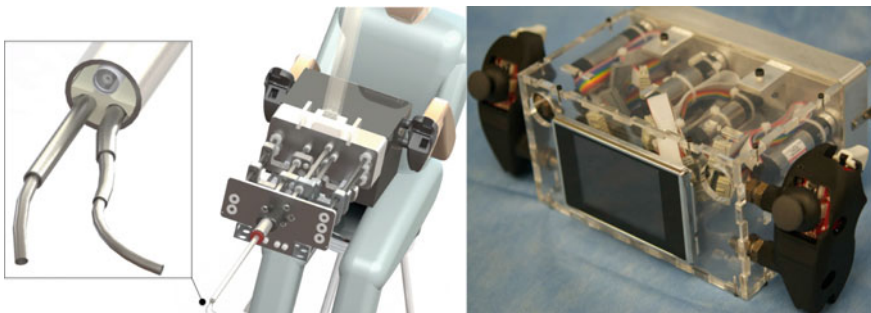


**Fig. 1** The surgeon has hand-held control of the entire system, which is supported by a counter-balanced arm (see Fig. 4). The surgeon controls each concentric tube manipulator with joysticks and triggers located on the handles shown in the right image above, based on endoscopic video feedback

benefits include a 50 % reduction in catheterization time, a 33 % reduction in hospitalization duration, and the elimination of the need for blood transfusion [8]. Recently, long term follow-up data has shown that HoLEP requires fewer re-operations, which is leading many in the urology community to conclude that HoLEP should become the new gold standard treatment for enlarged prostate [9].

Despite its clinical advantages, HoLEP is conducted in only a few institutions because it is extremely challenging for the surgeon [10]. It is physically demanding because large forces are required to angle the endoscope, due to the soft tissues surrounding it. To make matters worse, the surgeon must simultaneously manipulate soft tissue using the endoscope itself, and bring the laser fiber (which has no articulation, aiming straight out from the endoscope at a fixed position with respect to the image) to bear on the desired surgical target, which requires immense surgical skill.

The robotic system described in this paper is designed to alleviate these challenges. It passes curved, flexible continuum manipulators through the same endoscope currently used in the manual procedure, to enable the surgeon to aim the laser with one manipulator and retract tissue with the other. The hand-held nature of our system and integration of a standard clinical endoscope enables it to fit seamlessly into the current clinical workflow, which we believe will facilitate adoption by the medical community.

Toward our overall goal of making HoLEP easier to perform, the specific objectives of this paper are (1) to experimentally illustrate that the concentric tube robots can enable the surgeon to reach a larger portion of the desired resection ellipsoid in HoLEP, (2) to experimentally compare the accuracy of joint space and task space mappings from the surgeon's thumb and finger controls to concentric manipulator motions, and (3) to experimentally demonstrate the system in a realistic setting by laser resecting an anatomically accurate prostate model. We accomplish these objectives via a set of user studies with two experienced urologic surgeons.

## 2 Technical Approach

### 2.1 Robot Design

Our robotic system consists of three main modules: the user interface, the transmission, and the endoscope. Detailed design information can be found in [7]. Briefly, at the back of the robot is the user interface module, as shown in Fig. 1. This module is designed to quick connect to the transmission module through spring-loaded shaft couplings and houses nine brushless motors. Fixed to the outside of the user interface module are handles, where the surgeon grasps the robot and can manually manipulate the entire robot to control endoscope pose. Each handle has an embedded joystick and trigger, which are used for controlling the concentric tube manipulators. A screen is also placed between the surgeon's hands, which can be used to display the endoscopic view. Originally, we thought the surgeons may prefer to have the visualization inline with the tools they are manipulating. In practice, however, we

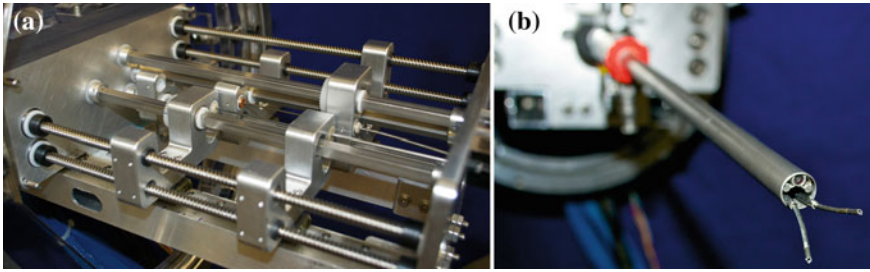


**Fig. 2** **a** The transmission section: square shafts transmit the torque to rotate the concentric tubes, while lead screws drive carriers which translate the tubes. **b** The rigid endoscope can be seen mounted to the front of the robot, with two concentric tube robots passing through it. Two fiber optic bundles surround the lens to provide illumination. The outer diameter of the endoscope is 8.3 mm, and the two manipulators pass through a single 5 mm port in it

have found surgeons tend to prefer large high definition screens in the operating room.

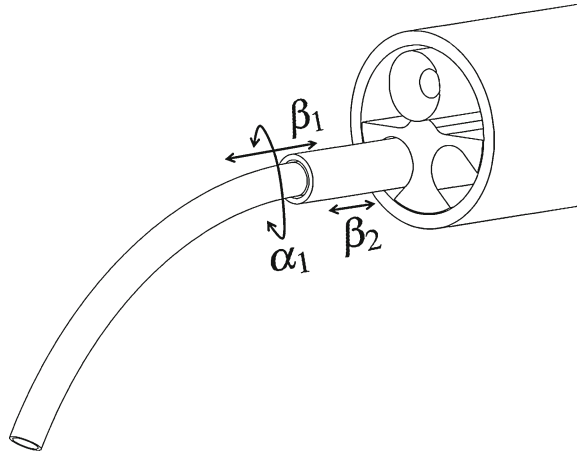
The transmission section, shown in Fig. 2, converts the motion of the motors in the user interface module into translation and rotation of the tubes. The transmission section is capable of driving 9 DOF. One arm was designed as a three tube, 6 DOF manipulator, while the other was designed as a two tube, 3 DOF manipulator (in the set of experiments described in this paper, however, both arms behave as 3 DOF manipulators). Linear motion of the tubes is achieved via lead screws, which drive tube carriers that ride on ball bearing blocks on a guide rail. Rotation of the tubes is achieved via square shafts, which transmit torque through a gear train to the tube.

We leverage the surgeon’s endoscopic manipulation skills and retain the current clinical workflow by designing this robot as a hand-held robot with a clinical endoscope (Storz, Inc. 27292 AMA, 26 Fr) mounted to the front of the transmission section, as shown in Fig. 2. Because this endoscope is rigidly mounted to the robot, manipulation of the robot via the user interface handles also manipulates the endoscope. This endoscope contains optics and light sources as well as a 5 mm tool channel, through which we pass our concentric tube robots. For a more detailed design description, see [7].

## 2.2 Concentric Tube Robots

Concentric tube robots are a class of continuum robots composed of concentrically nested, precurved, elastic tubes first proposed for use as robotic manipulators simultaneously in [11, 12]. They are typically made of superelastic nitinol, which is well suited for this application because it has 8% recoverable strain and can be shape set into desired curves while maintaining its superelasticity. When these precurved tubes are translated and rotated at their bases, their elastic interaction creates “tentacle-like” motion (elongation and bending) of the device. Geometrically exact mechanics-based

**Fig. 3** The actuation variables  $\alpha_1$ ,  $\beta_1$ , and  $\beta_2$  denote rotation of the inner tube, translation of the inner tube, and translation of the outer tube, respectively



models now exist for these manipulators [13, 14]. The manipulators used in the experiments in this paper are a special case concentric tube robot composed of two tubes: a nitinol inner tube with a constant curvature arc at its tip, and a straight, steel outer tube. Such a manipulator has three actuated degrees of freedom (see Fig. 3): rotation of the inner tube ( $\alpha_1$ ), translation of the inner tube ( $\beta_1$ ), and translation of the outer tube ( $\beta_2$ ). We approximate the outer tube as perfectly straight and rigid, which allows the kinematics to be computed purely geometrically, the details of which can be found in [7].

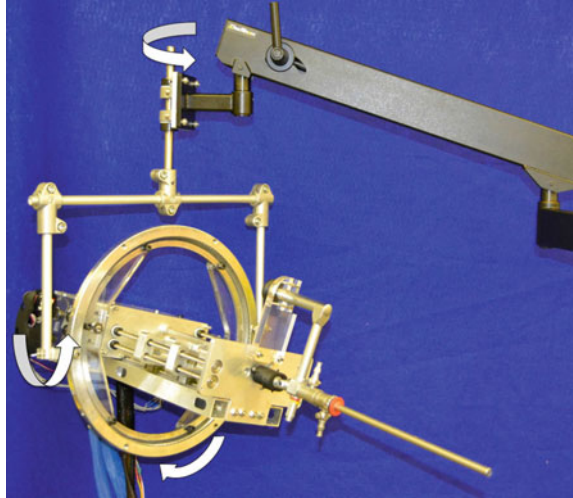
### 2.3 Counterbalance System

To assist the surgeon by supporting the weight of the the hand-held robot (while still permitting 6 DOF motion) a counterbalanced arm (Dectron, USA) is provided (Fig. 4). As the robot is used in transurethral endoscopic prostate surgery, the endoscope approximately operates through an anatomically constrained center of motion near the apex of the prostate. This constraint is created by the soft tissue pressure provided by the urogenital diaphragm. Thus, the surgeon must manually control 4 DOF (roll, pitch, yaw, and insertion).

### 2.4 User Interface Mappings

The introduction of concentric tube robots adds additional degrees-of-freedom for the surgeon. As illustrated in Fig. 1, the concentric tube robots add 9 DOF, three on the two-tube arm and six on three-tube arm. However, in the set of experiments described in this paper, for simplicity, both arms were configured as identical two-

**Fig. 4** A counterbalanced arm allows for manual 6-DOF spatial positioning of the robot by the surgeon



tube, 3 DOF manipulators. Thus, in our experiments, we assess the surgeon's ability to coordinate 10 DOF based on the endoscopic view. The surgeon manipulates the concentric tube robots via the embedded joystick (with pushbutton capability) under his/her thumb and an analog trigger under his/her index finger.

Initially, likely due to familiarity with manipulating manual tools through endoscope ports, surgeons expected to prefer direct joint space control of the rotation and axial extension of the tubes. Furthermore, in task space control, surgeons were initially surprised by rapid robot motions near singularities, and perceived these as a lack of control of the robot. Based on this, we implemented both joint and task space control and set out to experimentally compare the two.

In joint space control, the index finger trigger was mapped to rotational velocity of the inner tube ( $\dot{\alpha}_1$ ), and upward motion of the joysticks (on each handle) were mapped to translational velocity of the tubes ( $\dot{\beta}_1, \dot{\beta}_2$ ). The surgeon was able to reverse the direction of rotation by clicking the joystick and then again depressing the index finger trigger. All commanded velocities were linearly proportional to the deflection of the relevant analog input from thumb joysticks and index finger triggers.

In task space control, the tips of the manipulators move relative to the camera frame using a resolved rates algorithm. Thumb joystick deflections were mapped to end-effector velocity in the plane of the endoscopic view. The index finger trigger was mapped to end effector velocity perpendicular to the image plane, and clicking the joystick reversed the direction of motion perpendicular to the image plane (Fig. 5).

### 3 Experiments

Three distinct experiments were conducted: (1) to evaluate the ability of the concentric tube robots to access more of the prostate than a straight rigid endoscope, (2) to

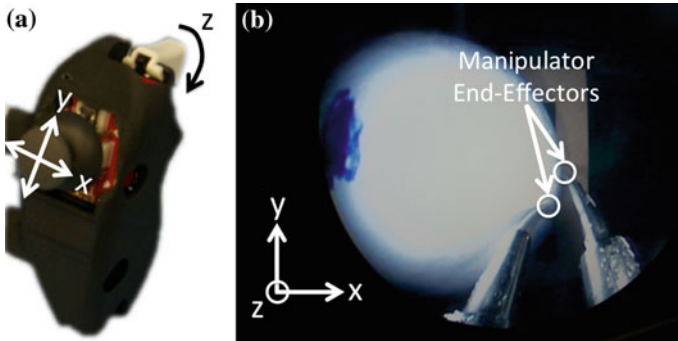


**Fig. 5** **a** One of the handles that comprise the user interface, illustrating an analog joystick (with pushbutton) and trigger. The joystick provides for two bidirectional inputs, and the trigger gives a third unidirectional input. The pushbutton is used to reverse the direction of the trigger input. **b** The endoscopic view

compare the tracking ability of the hand-held system in task space and joint space, and (3) to show that this robotic system can perform the realistic laser resections required for this surgery.

### ***3.1 Prostate Surface Access with Concentric Tube Robots***

To approximate the center of motion (which in humans comes from anatomical constraints as mentioned earlier) in a benchtop setting, we used a wooden support with a hole through it, positioned at an anatomically accurate distance from the prostate model. To simulate the surgeon's desired surface for laser resection in HoLEP, we affixed an ellipsoid of anatomically correct dimensions (30 mm × 42 mm × 47 mm [15]) made of hard plastic behind this center of motion as shown in Fig. 6.

An Aurora Electromagnetic Measurement System (Northern Digital Inc.) was registered to the test stand, and an electromagnetic tracking coil was embedded in the tip of the concentric tube robot. Two experienced urologic surgeons then used the system to scan the surface of the desired resection ellipsoid. One two-tube, three DOF manipulator was used under both joint space and task space control and the surgeons scanned one quadrant of the model (the model is axially symmetric, so the ability to scan one quadrant demonstrates ability to scan all). The intent of this simple experiment was to compare the kinematic ability of this system against the straight, rigid endoscope which is currently used clinically, and to see if there were any differences between task space and joint space control in terms of resection surface accessibility when tissue deformation is not present. This experiment was completed prior to the design of the counterbalanced arm, so a passive lockable mechanical arm was used to support the robot. It was locked in place during the experiment, but the

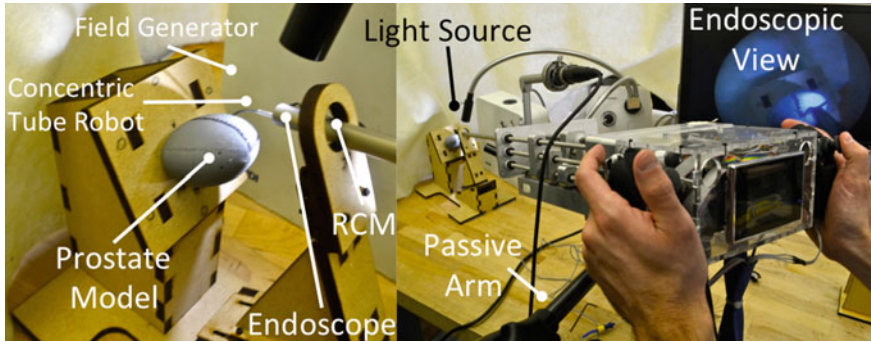


**Fig. 6** The experimental setup constrains the endoscope to operate through a remote center of motion which would be anatomically constrained in a patient—we simulate the constraint here with a hole through a piece of wood. The surgeon scans the desired resection surface (the surface of the plastic model) with the instrument tip using endoscopic video feedback. The instrument tip is magnetically tracked

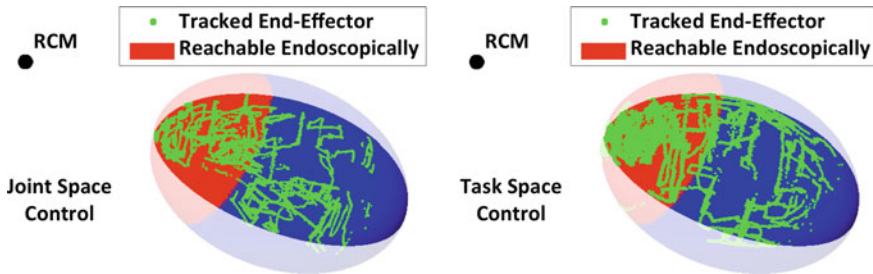
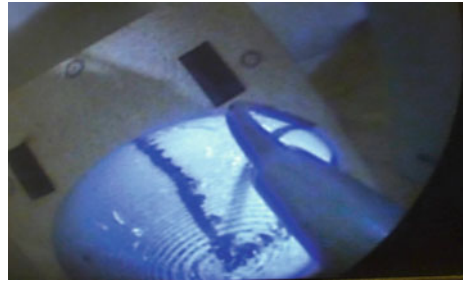


**Fig. 7** Magnetic tracking data showing the positions on the prostate surface accessed by two surgeons using the system in joint space mode (*left*) and task space mode (*right*). The *red region* indicates the best-case scenario for the surface reachable by a conventional endoscope (without tissue deformation), since it is only capable of a straight-line approach

surgeons were allowed to unlock it and reposition the entire robot whenever desired, before re-locking it and continuing with the experiment.

The experimental results are shown in Fig. 7. A cannula tip point was considered to be on the surface of the resection ellipsoid if the point was <2 mm from the surface. The figure shows the tracked points projected onto the closest point on the resection surface model. Figure 7 illustrates that surgeons were able to access nearly the entire available ellipsoidal surface of the prostate model with both control mappings, and a typical endoscope image during the experiment is shown in Fig. 8. The area reached by the robot represents an improvement of approximately 65% versus the best-case geometrically reachable area of existing straight, rigid clinical endoscopes without tissue deformation. This experiment shows that our robot is capable of reaching points relevant to prostate resection in a static case without tissue deformation, which is conservative, since tissue deformation tends to help make more points accessible rather than fewer. However, what it did not explore were quantitative differences

**Fig. 8** Endoscopic view of a surgeon scanning the resection surface model as would be required for laser dissection



between joint and task space operation which inspired the experiment in the following section.

### 3.2 Task Space Versus Joint Space Performance Comparison

To explore the differences between task space and joint space operation, a second experiment was conducted using the same experimental setup described in Sect. 3.1. However, rather than scanning an entire quadrant of the prostate, the surgeons were asked to follow a specific curve along the surface of the prostate model. The surgeons were instructed to stay as close to the path as possible throughout the experiment, and task completion time was recorded. This experiment was conducted using the counterbalanced arm shown in Fig. 4. It was done once with the arm unlocked (so that the surgeons could position and orient the endoscope as well as the concentric tube manipulators) and once with the arm locked (forcing the surgeons to use only the concentric tube manipulators without changing the overall endoscope pose). The paths were slightly different for the two scenarios and can be seen in Fig. 9.

The path shown in Fig. 9a was traced with counterbalance assistance by two surgeons, each using both control modes on separate trials, each performing two trials per mode, yielding a total of eight experimental runs. The main experimental results are in Table 1. The mean accuracy for both control modes with counterbalance

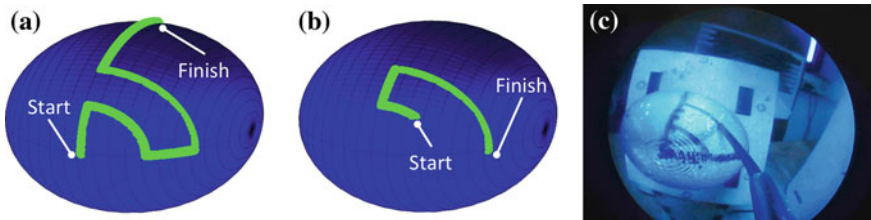


**Fig. 9** **a** Desired path of concentric tube robot tip for the experiment with free endoscope manipulation. **b** Desired path of concentric tube robot tip for the experiment with a fixed endoscope pose. **c** Concentric tube robot following the desired path on the prostate resection surface model

**Table 1** Counterbalanced tracing experiment (path shown in Fig. 9a)

	Joint space	Task space
Mean error (mm)	1.5	1.6
Max error (mm)	6.4	4.3
Time (s)	70.2	41.9

assistance was not significantly different for joint space control and task space control. The maximum tracked error (averaged over the eight runs) using joint space control was 6.4 mm, while it was only 4.3 mm when using task space control. Moreover, the total time to complete the task was almost twice as high using joint space control than task space control.

These results indicate that surgeons were capable of using both control modes to follow the prescribed path, but that while doing so in joint space mode, they occasionally made large errors. To explore this further, we examined the total time that the surgeons spent in a state of large error. In joint space mode, 5.4, 2.6, 1.9, and 1.0% of task completion time was spent in excess of 3 mm, 4 mm, 5 mm, and 6 mm error, respectively. In task space mode, 5.4% of task completion time was spent in excess of 3 mm, and error rarely exceeded 4 mm (0.2% of the time).

Noting qualitatively that surgeons were using substantial endoscope manipulation—particularly when employing joint space control, we performed another similar experiment in which we fixed the endoscope position and orientation by locking the counterbalanced support arm. Surgeons were then asked to trace the path shown in Fig. 9b. Again, two surgeons attempted to complete this task in both control modes, twice each per mode, for a total of eight experimental runs.

The results for task space control were similar for this experiment compared to when the endoscope had free motion. The maximum error (averaged over the four runs) was 4.0 mm. The only significant difference without endoscope manipulation was that it took surgeons longer to trace a given path length. More specifically, it took them approximately the same amount of time to trace a shorter path in this experiment than it did to trace the longer path in the experiment with free endoscope manipulation.

In sharp contrast, completion of the task was not achievable using joint space control with a fixed endoscope. On all four runs, the experiment was ended at surgeon request after an average time of 2 min, with over 15% of the time spent with >3 mm error (Table 2). We believe this indicates that the joint space control mapping was too mentally challenging for the surgeons to process rapidly or accurately without the assistance of endoscope pose manipulation, and that they were primarily using pose manipulation to trace the path in the corresponding experiment with free endoscope manipulation.

Considering all of the above experiments together, it appears that when using task space control, surgeons rely on a combination of endoscope pose manipulation and concentric tube manipulation to accomplish the task. In contrast, when using joint space control the surgeons appear to rely heavily on endoscope manipulation and use

**Table 2** Fixed endoscope tracing experiment (path shown in Fig. 9b)

	Task space
Mean error (mm)	1.6
Max error (mm)	4.0
>3 mm error (%)	4.1
>4 mm error (%)	1.7
Time (s)	40.3

The task was not achievable in joint space mode. Surgeons attempted it for an average of 2 min per trial in joint space mode before requesting that the experiment be ended

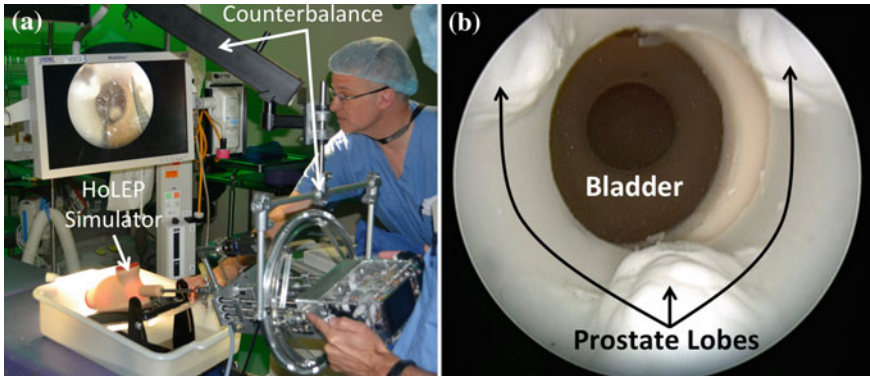


**Fig. 10** **a** The counterbalanced robot operates transurethral through the HoLEP simulator. The surgeons visually servo the concentric tube manipulator tips in task space with high definition endoscopic video feedback. **b** The endoscopic view shows the three lobes of the synthetic prostate. Each surgeon was tasked with laser resecting one lobe of the prostate phantom

little concentric tube robot manipulation to accomplish the task. It is also interesting to note that when using task space control, endoscope pose manipulation enables an increase in the speed of motion, without negatively impacting the accuracy of the manipulation. In future experiments we intend to encode the endoscope pose itself, to more deeply study these qualitative observations that appear to be consistent with the data collected.

### 3.3 Laser Resection of an Anthropomorphic Prostate Phantom

In this experiment we used a TruLase Prostate HoLEP simulator (TPR100, TruCorp Ltd.) designed for training surgeons in HoLEP (see Fig. 10). This simulator is anatomically accurate and allows for laser enucleation of a synthetic prostate specimen in a fluid-filled environment similar to that of HoLEP surgery. In this experiment, the surgeon used both concentric tube manipulators with task space control. A 500  $\mu\text{m}$

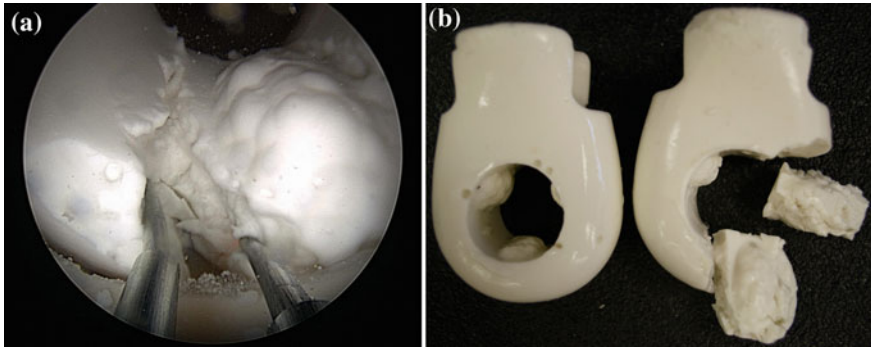


**Fig. 11** **a** The left manipulator retracts the tissue, exposing the targets for the right manipulator to cut with the holmium laser. **b** A photograph of what the prostate model looked like before and after the experiment

holmium laser fiber was passed through the inner tube of the right concentric tube manipulator, while the left manipulator was used for tissue retraction with a clear inner lumen. Both manipulators were identical two-tube, 3-DOF devices, as shown in Fig. 3 with tube curvatures of  $30 \text{ m}^{-1}$ .

The simulator was filled with saline solution and endoscopic saline irrigation was used in the same manner as in a clinical HoLEP procedure. The synthetic prostate used in this experiment was the three lobe prostate insert (TPRO-03, TruCorp Ltd.) as shown in Fig. 10. A clinical 80 W holmium laser was used, and the surgeon could fire the laser on demand using a foot pedal, just as they would in a current clinical HoLEP case. The counterbalance arm was used and the endoscope (and robot) were free to be spatially oriented as desired. Surgeons were asked to laser resect and remove a single lobe of the prostate, and push it into the bladder, just as they would in a current clinical HoLEP case (the specimen then gets morcellated within the bladder in the current clinical HoLEP procedure, and our system is designed to follow the same protocol for specimen removal). There were no restrictions or instructions regarding use of robotic manipulators versus manual endoscopic placement; surgeons were free to use the device as they wished.

Two lobes were successfully laser resected from the prostate model and pushed into the bladder, one by each surgeon. One surgeon removed the median lobe (the lobe in the center of Fig. 10b), while the other removed one of the lateral lobes. The post-experiment synthetic prostate model can be seen in Fig. 11. After a short learning curve in which the surgeons focused primarily on the laser arm, surgeons began to use coordinated movement of both arms, increasingly relying on retraction from the retraction arm. The retraction arm was used to expose desired targets within tissue and the laser arm to cut the exposed surface with the laser.

## 4 Conclusions

Several important experimental insights have emerged from this series of experiments. First, we have shown that without tissue deformation our robotic system enables the surgeon to reach significantly more of the desired resection surface than is possible using a standard endoscope, regardless of the control mapping (see Fig. 7). These results indicate that our system may be able to reduce the amount of tissue deformation required in the procedure (both prostate tissue and surrounding tissues). If so, this would reduce the physical demands of the procedure on the surgeon, and reduce the technical challenge of the procedure associated with simultaneously deforming the prostate and aiming the laser with the same device.

We also sought to compare joint space control with task space control in terms of tracking accuracy. The primary motivation for this was the surgeon's initial inclination toward joint control due to their familiarity inserting other tools through endoscope ports manually, combined with their reluctance to see the robot move rapidly near singularities. Our primary observations were:

- (1) With free endoscope movements, surgeons are likely to be able to complete the procedure, regardless of control mapping. This makes sense, since highly skilled surgeons can complete the procedure (albeit with significant difficulty) with a straight endoscope and no laser articulation. With free endoscope manipulation, joint and task space control yielded similar tip accuracy, with task space control enabling more rapid completion of the experiment.
- (2) When surgeons were required to use the concentric tube manipulators exclusively (endoscope pose fixed), surgeons were able to follow complex curves accurately using task space control, but were unable to do so (or even complete the experiment) with joint space control.

These results lead us to believe that surgeons tend to primarily use endoscope motion rather than concentric tube robot motion when performing the task with free endoscope motion while using joint space control. Anecdotally, surgeons also found that their comfort level with task space control increased rapidly through performing these experiments, and they observed that robot motions, while sometimes fast, were predictable.

The prostate phantom resection experiment illustrated our robotic system functioning in a realistic model of clinical conditions. It also showed the surgeons could simultaneously coordinate many degrees of freedom, including controlling the pose of the endoscope while simultaneously using two concentric tube manipulators. We also observed that the learning curve for doing so was short for surgeons experienced in endoscopic surgery. Qualitatively, we observed that coordinated use of two arms made the procedure significantly easier, since one arm could be used to retract tissue and expose sites for the other to cut with the laser.

There remain many ways to improve the system in the future. Perhaps most importantly, surgeons observed that they would like to work as close as possible to the endoscope tip with the concentric tube manipulators. We explored this problem

in [16], where we showed that it is possible to significantly expand the portion of the endoscope view that can be accessed by the concentric tube robots by enabling them to emerge and begin to curve a short distance behind the tip of the endoscope. We intend to implement this change and continue to iteratively refine the user interface and robotic hardware as we move forward toward cadaver experiments.

**Acknowledgments** This work was funded in part by the National Science Foundation (NSF) under IIS-105433, in part by the National Institutes of Health (NIH) under R01 EB017467, and in part by the Vanderbilt Initiative in Surgery and Engineering. The content is solely the responsibility of the authors and does not necessarily represent the official views of the NSF or NIH.

## References

1. Davies, B.L., Hibberd, R.D., Ng, W.S., Timoney, A.G., Wickham, J.E.A.: The development of a surgeon robot for prostatectomies. *Proc. Inst. Mech. Eng Part H: J. Eng. Med.* **205**, 35–38 (1991)
2. Davies, B.: Medical robotics—a bright future. *Lancet* **368**, S53–S54 (2006)
3. Ho, G., Ng, W.S., Teo, M.Y., Kwok, C.K., Cheng, W.S.C.: Experimental study of transurethral robotic laser resection of the prostate using the LaserTrode lightguide. *J. Biomed. Opt.* 244–251 (2001)
4. de Badajoz, E.S., Garrido, A.J., Vacas, F.G., Martinez, V.F.M., de Gabriel, J.G., Lozano, J.F., Cerezo, A.G.: New master arm for transurethral resection with a robot. *Archivos Espanoles de Urologia* **55**, 1.247–1.250 (1998)
5. Hashimoto, R., Kim, D., Hata, N., Dohi, T.: A tubular organ resection manipulator for transurethral resection of the prostate. In: *IEEE/RSJ International Conference on Intelligent Robots and Systems*, pp. 3954–3959 (2004)
6. Goldman, R.E., Bajo, A., MacLachlan, L.S., Pickens, R., Herrell, S.D., Simaan, N.: Design and performance evaluation of a minimally invasive telerobotic platform for transurethral surveillance and intervention. *IEEE Trans. Biomed. Eng.* **60**(4), 918–925 (2013)
7. Hendrick, R.J., Herrell, S.D., Webster III, R.J.: A Multi-arm hand-held robotic system for transurethral laser prostate surgery. In: *IEEE International Conference on Robotics and Automation*, pp. 2850–2855 (2014)
8. Ahyai, S.A., Lehrich, K., Kuntz, R.M.: Holmium laser enucleation versus transurethral resection of the prostate: 3-Year follow-up results of a randomized clinical trial. *Eur. Urol.* **52**(5), 1456–1463 (2007)
9. van Rij, S., Gilling, P.J.: In 2013 Holmium laser enucleation of the prostate (HoLEP) may be the new ‘Gold Standard’. *Curr. Urol. Rep.* **13**, 427–432 (2012)
10. Lingeman, J.E.: Holmium laser enucleation of the prostate—if not now, when? *J. Urol.* **186**(5), 1762–1763 (2011)
11. Webster III, R.J., Okamura, A., Cowan, N.J.: Toward active cannulas: miniature snake-like surgical robots. In: *IEEE/RSJ International Conference on Intelligent Robots and Systems*, pp. 2857–2863 (2006)
12. Sears, P., Dupont, P.: A Steerable needle technology using curved concentric tubes. In: *IEEE/RSJ International Conference on Intelligent Robots and Systems*, pp. 2850–2856 (2006)
13. Rucker, D.C., Jones, B.A., Webster III, R.J.: A geometrically exact model for externally loaded concentric-tube continuum robots. *IEEE Trans. Robot.* **26**(5), 769–780 (2010)
14. Dupont, P.E., Lock, J., Itkowitz, B., Butler, E.: Design and control of concentric-tube robots. *IEEE Trans. Robot.* **26**(2), 209–225 (2010)

15. Leenstra, J.L., Davis, B.J., Wilson, T.M., Mynderse, L.A., Herman, M.G., Hillman, D., Allen, K., Cheville, J., Holmes, D., King, B.: Prostate dimensions and volume in 700 patients undergoing primary surgical or radiotherapeutic management of localized adenocarcinoma: implications for design of minimally invasive prostate cancer devices. *Int. J. Radiat. Oncol.* **69**(3), S380–S381 (2007)
16. Hendrick, R.J., Mitchell, C.R., Herrell, S.D., Webster III, R.J.: Concentric tube robots for transurethral prostate surgery: matching the workspace to the endoscopic field of view. In: *The Hamlyn Symposium on Medical Robotics* (2014)